Fluid Phase Equilibria 448 (2017) 69–80

Contents lists available at ScienceDirect

Fluid Phase Equilibria

journal homepage: www.elsevier.com/locate/fluid

Measurement and PC-SAFT modeling of solid-liquid equilibrium of deep eutectic solvents of quaternary ammonium chlorides and carboxylic acids

Paula V.A. Pontes [a, 1], Emanuel A. Crespo [b, c, 1], Mónia A.R. Martins [a, b], Liliana P. Silva [b], Catarina M.S.S. Neves [b], Guilherme J. Maximo [a], Miriam Dupas Hubinger [a], Eduardo A.C. Batista [a], Simão P. Pinho [d], João A.P. Coutinho [b], Gabriele Sadowski [c], Christoph Held [c, *]

[a] Faculty of Food Engineering, University of Campinas, 13083-862 Campinas, São Paulo, Brazil
[b] CICECO – Aveiro Institute of Materials, Department of Chemistry, University of Aveiro, 3810-193 Aveiro, Portugal
[c] Laboratory of Thermodynamics, Department of Biochemical and Chemical Engineering, TU Dortmund, 44227 Dortmund, Germany
[d] Associate Laboratory LSRE-LCM, Departamento de Tecnologia Química e Biológica, Instituto Politécnico de Bragança, 5301-857 Bragança, Portugal

ARTICLE INFO

Article history:
Received 30 January 2017
Received in revised form
6 April 2017
Accepted 14 April 2017
Available online 20 April 2017

Keywords:
Melting properties
Thermodynamics
Tetra alkyl ammonium salts
Fatty acids
Phase diagrams

ABSTRACT

In this study the solid-liquid equilibria (SLE) of 15 binary mixtures composed of one of three different symmetrical quaternary ammonium chlorides and one of five different fatty acids were measured. The experimental data obtained showed extreme negative deviations to ideality causing large melting-temperature depressions (up to 300 K) that are characteristic for deep eutectic systems. The experimental data revealed that cross-interactions between quaternary ammonium salt and fatty acid increase with increasing alkyl chain length of the quaternary ammonium chloride and with increasing chain length of the carboxylic acid. The pronounced decrease of melting temperatures in these deep eutectic systems is mainly caused by strong hydrogen-bonding interactions, and thermodynamic modeling required an approach that takes hydrogen bonding into account. Thus, the measured phase diagrams were modeled with perturbed-chain statistical associating fluid theory based on the classical molecular homonuclear approach. The model showed very good agreement with the experimental data using a semi-predictive modeling approach, in which binary interaction parameters between quaternary ammonium chloride and carboxylic acid correlated with chain length of the components. This supports the experimental findings on the phase behavior and interactions present in these systems and it allows estimating eutectic points of such highly non-ideal mixtures.

1. Introduction

Aiming at sustainable process design and taking into account the growing focus on green chemistry, there has been an effort towards the development of novel and environmentally friendly solvents with equivalent or better performance than classical organic solvents. Such novel solvents are supercritical CO_2, ionic liquids (ILs), and, more recently, also deep eutectic solvents (DES).

Firstly proposed by Abbott and co-workers [1], DES belong to a neoteric class of eutectic solvents formed by mixtures of two (or more) compounds, resulting from hydrogen bond complexation between the mixture compounds, with a eutectic point far below the melting points of the individual components [2]. DES can be easily prepared by mixing the components at a moderate temperature, without chemical reactions or complex purification steps. Many DES can be prepared using cheap and well-characterized biodegradable materials, making the "synthesis" green and safe [2,3]. They may also be classified as designer solvents since their structures can be adjusted by selecting the hydrogen-bond donor–acceptor combinations, tailoring their phase behavior and physical properties [4]. Moreover, it was shown that addition of agents able to break the DES complex allows recrystallization and

* Corresponding author.
E-mail address: Christoph.Held@bci.tu-dortmund.de (C. Held).
[1] P.V.A.P. and E.A.C. contributed equally.

http://dx.doi.org/10.1016/j.fluid.2017.04.007
0378-3812/

recovery of one or both of the initial components, since these remain in their molecular state upon melting [5,6].

DES exhibit a wide range of properties which make them an attractive family of solvents for different applications in catalysis, organic synthesis, dissolution and extraction processes, electrochemistry and material chemistry [2–5,7,8]. The [Ch]Cl:urea mixture (1:2 mol), for example, was used in the Perkin condensation of cinnamic acid [9], reduction of epoxides [10] or in an electrophilic substitution of quinone derivatives [11]. Other applications are the incorporation of metal ions in solution for metal deposition and electro polishing [3], metal extraction [12], conversion of lignocellulosic biomass [13], gas separations [14], extraction of glycerol from biodiesel [15], extraction media for azeotropic mixtures [16], fuel purification [17], potential drug vehicles [18], or in the preparation of nanomaterials [19].

The low toxicity, non-volatility, non-flammability and non-reactivity with water, along with their renewable, and biodegradable character, and the wide availability of precursors, are some of the favorable characteristics of these compounds [2,20]. The renewability of a DES depends mainly on its starting materials being most of the DES described in literature prepared using abundant natural compounds. The most common precursors are quaternary ammonium salts, particularly choline chloride, due to its non-toxicity, biodegradability and economic synthesis, combined with polyols, urea, carboxylic acids, sugars or other safe hydrogen bond donors. Monocarboxylic acids with long aliphatic chains, known as fatty acids, are the major co-products of the vegetable oils refining. Their use in DES would have a positive impact on the processes sustainability since, besides their vast natural sources, they allow purification of the extracts when used as solvents for extraction operations [21].

While much work has been reported using these novel solvents, the number of DES which are liquid at room temperature is still very limited. Moreover, data on their solid-liquid equilibria (SLE) is surprisingly scarce despite the important information it provides on the operation window (range of compositions and temperatures) as well as on donor-acceptor interactions in these systems. Likewise, modeling the SLE by suitable equations of state (EoS) and/or activity coefficient models is a poorly explored research field due to both, lack of enough comprehensive and reliable experimental data and the strong and highly complex interactions between the DES constituents that are not easily captured by most models.

In the past few years, Statistical Associating Fluid Theory (SAFT), a molecular-based model that accounts for the repulsive and attractive interactions of fluids [22,23], has been used to successfully describe a wide variety of systems [24,25]. Additionally, Perturbed-Chain SAFT (PC-SAFT) [26], the most prominent modification of original SAFT, was already successfully applied to systems containing DES. Verevkin et al. [27] used PC-SAFT to model infinite dilution activity coefficients of 23 different solutes in [Ch]Cl:glycerol and Zubeir et al. [28] used PC-SAFT to model the CO_2 solubility in quaternary ammonium salts + lactic acid mixtures.

In this context, the purpose of this work is to measure the solid-liquid phase diagrams of fifteen new DES composed of one quaternary ammonium salt [tetramethylammonium chloride ([N_{1111}]Cl), tetraethylammonium chloride ([N_{2222}]Cl) and tetrapropylammonium chloride ([N_{3333}]Cl)] and of one fatty acid (capric acid, lauric acid, myristic acid, palmitic acid or stearic acid) that are commonly found in vegetable oils. PC-SAFT is here applied for the first time to describe the DES solid-liquid phase diagrams by fitting energy related binary interaction parameters to the measured experimental data allowing to obtain information about the non-ideality of the compounds in the liquid phase and new insights regarding the hydrogen-bonding interactions between the DES constituents.

2. Materials and methods

2.1. Chemicals

The quaternary ammonium salts (hydrogen-bond acceptor, HBA) and the fatty acids (hydrogen-bond donor, HBD) used to prepare the DES are described in Table 1. The quaternary ammonium salts were dried under vacuum at room temperature during at least three days while fatty acids were used as received from the supplier. A Metrohm 831 Karl Fischer coulometer using the analyte Hydranal®—Coulomat AG, from Riedel-de Haën, was used to determine the water content of the dried salts, which was found to be 927, 368 and 418 ppm respectively for [N_{1111}]Cl, [N_{2222}]Cl, [N_{3333}]Cl. Indium, used for the DSC calibration, was supplied by PerkinElmer with a purity higher than 0.999 (molar fraction).

2.2. Methods

2.2.1. Solid liquid equilibria

Mixtures of the HBA-HBD were prepared in the whole composition range, allowing the measurement of the solid-liquid phase diagrams. Three different experimental methodologies were used, the visual method, the melting points measurements methods, and differential scanning calorimetry. These are explained in the following.

For the visual method, binary mixtures were weighted at room temperature using an analytical balance model ALS 220-4N from Kern with an accuracy of ±0.002 g, inside a dry-argon glove-box. Vials with the mixtures were heated in an oil bath under stirring using a heating plate until complete melting prior to recrystallization. After the first cycle the melting temperatures corresponding to the last crystal disappearance were recorded. The temperature was measured with a Pt100 probe with a precision of ±0.1 K. This procedure was repeated at least two times.

For measurements of the melting points, samples were prepared as described in the visual method procedure. After recrystallization, solid mixtures were ground in the glove-box and the powder was filled into a capillary. Melting temperatures were then determined with an automatic glass capillary device model M-565 from Büchi (100–240 V, 50–60 Hz, 150 W, temperature resolution: 0.1 K). A temperature gradient of 0.5 K min^{-1} was used and the melting points measurements were repeated at least two times.

Differential Scanning Calorimetry (DSC) was applied in specific cases indicated in Tables S1, S2, and S3. Mixtures were prepared into a glass vessel on an analytic balance XP205 (Mettler Toledo, precision = 2×10^{-4} g) in a glove box under inert nitrogen atmosphere (purity ≥ 0.99996 mass fraction). The mixtures were melted under stirring on a heating plate until a homogeneous liquid mixture was obtained, and the mixture then cooled at room temperature. Samples (2–5 mg) were hermetically sealed in aluminum pans inside the glovebox and then weighed in a micro analytical balance AD6 (PerkinElmer, USA, precision = 2×10^{-6} g). A DSC 2920 calorimeter (TA Instruments) working at atmospheric pressure and coupled to a cooling system was used for the sample analysis. The method was based on a cooling run at 5 $K \cdot min^{-1}$ until 208.15 K followed by a heating run with a rate of 1 $K \cdot min^{-1}$ until 10 K above melting. Nitrogen (purity ≥ 0.99999 mass fraction) was used as purge gas. The melting temperatures of the samples were assumed to be the maximum temperatures of the melting peak, taking into account the appearance of broad thermo events in the melting of the eutectic mixtures (see Fig. S1). Data were analyzed through the TA Universal Analysis software (TA Instruments). For pure compounds, the uncertainty of the equilibrium data was calculated by the average of the standard deviations of triplicates. The equipment was previously calibrated with indium.

Table 1
Sources and purities of the compounds used in this work.

Component	Molecular Formula	CAS number	Supplier	Purity (mass %)[a]
HBA (Quaternary Ammonium Salts)				
$[N_{1111}]Cl$	$C_4H_{12}ClN$	75-57-0	Sigma-Aldrich	97.0
$[N_{2222}]Cl$	$C_8H_{20}ClN$	56-34-8	Sigma-Aldrich	98.0
$[N_{3333}]Cl$	$C_{12}H_{28}ClN$	5810-42-4	Sigma-Aldrich	98.0
HBD (Fatty Acids)				
Capric acid	$C_{10}H_{20}O_2$	334-48-5	Sigma	≥99.0
Lauric acid	$C_{12}H_{24}O_2$	143-07-7	Sigma	≥99.0
Myristic acid	$C_{14}H_{28}O_2$	544-63-8	Sigma	≈95.0
Palmitic acid	$C_{16}H_{32}O_2$	57-10-3	Aldrich	≥98.0
Stearic acid	$C_{18}H_{36}O_2$	57-11-4	Merck	≥97.0

[a] According to the supplier.

2.2.2. Water activities of the quaternary ammonium chlorides

Water activities (a_w) measurements were carried out using a Novasina hygrometer LabMaster-a_w (Lucerne, Switzerland) with an accuracy of $0.001a_w$ and ±0.20 K in the controlled temperature chamber. The instrument principle is based on resistive-electrolytic method. The equipment was initially calibrated with six saturated pure salt standard solutions (water activity ranging from 0.113 to 0.973), provided by the supplier. Moreover, in order to achieve the given accuracy, a calibration curve was built using at least six aqueous solutions of LiCl or NaBr at different salt molalities and results were compared to those recommended by Refs. [29] and [30], respectively. Quaternary ammonium solutions were prepared at room temperature by mixing salts and water at the desired composition. The water content is presented in Table S4. Samples of approximately 2–3 cm^3 were then filled into proper cells and placed in the air-tight equilibrium chamber. When a constant value was reached, the water activity was recorded. Usually, solutions reached equilibrium in less than 1 h.

2.2.3. Density of mixtures water + quaternary ammonium chloride

The density measurements were performed at atmospheric pressure and in the temperature range from 298.15 to 358.15 K using an automated SVM 3000 Anton Paar rotational Stabinger viscometer–densimeter (temperature uncertainty: ± 0.02 K; absolute density uncertainty: $\pm 5 \times 10^{-4}$ g cm^{-3}). The solutions prepared for the water activity measurements were used here. The salt content of the samples and the resulting mixture densities are presented in Tables S5–S7.

3. Thermodynamic modeling

3.1. PC-SAFT EoS

SAFT is a thermodynamic approach derived from Wertheim's first-order thermodynamic perturbation theory [31–34], proposed by Chapman and co-workers [22,23]. Since the original SAFT version, several modifications have been proposed. In particular, PC-SAFT proposed by Gross and Sadowski in 2001 [26] that uses a system of freely jointed hard spheres as reference (designated as hard-chain system), which may be perturbed by dispersive and association interactions. The PC-SAFT model attracted much attention from researchers since it was already successfully applied to a wide variety of systems. Compared to the original SAFT model, PC-SAFT modeling results demonstrate good improvements of long-chain molecules, like polymers or ILs, and even of substances of low molecular weight [26,35].

In general, SAFT-type equations are written in terms of residual molar Helmholtz energy, a^{res}, defined as the difference between the total molar Helmholtz energy and that of an ideal gas at the same temperature and molar density:

$$\frac{a^{res}}{RT} = \frac{a}{RT} - \frac{a^{id}}{RT} \tag{1}$$

The residual Helmholtz energy is, in PC-SAFT, defined as the sum of different contributions from different molecular forces:

$$\frac{a^{res}}{RT} = \frac{a^{hc}}{RT} + \frac{a^{disp}}{RT} + \frac{a^{assoc}}{RT} \tag{2}$$

In Equation (2), the superscripts refer to the terms accounting for the residual, hard-chain fluid, dispersive and associative interactions, respectively. An EoS written in terms of the Helmholtz energy has the advantage that the calculation of all the thermodynamic properties is possible by using only derivatives and ideal-gas integrals.

In the PC-SAFT framework, a non-associating component i is characterized by three-pure component parameters, namely the segment number, m_i^{seg}, the segment diameter, σ_i, and the van der Waals dispersion energy parameter between two segments, u_i. For associating components, two additional parameters are required, namely the association-energy parameter, ε^{AiBi}, and the association-volume parameter, κ^{AiBi}. Additionally, a proper association scheme specifying number/type and allowed interactions has to be assigned to each associating component.

When describing mixtures, the conventional Lorenz-Berthelot combining rules were used to determine the mixture parameters where one adjustable binary interaction parameter, k_{ij}, for correction of the cross-dispersion energy can be used whenever required.

$$\sigma_{ij} = \frac{1}{2}(\sigma_i + \sigma_j) \tag{3}$$

$$u_{ij} = (1 - k_{ij})\sqrt{u_i u_j} \tag{4}$$

Simple combining rules for the cross-association interactions between the two components, proposed by Wolbach and Sandler [36], were further applied when dealing with mixtures.

$$\varepsilon^{AiBj} = \frac{1}{2}\left(\varepsilon^{AiBi} + \varepsilon^{AjBj}\right)(1 - k_{ij\_eps}) \tag{5}$$

$$\kappa^{AiBj} = \sqrt{\kappa^{AiBi} \cdot \kappa^{AjBj}}\left(\frac{\sqrt{\sigma_{ii} \cdot \sigma_{jj}}}{1/2\,(\sigma_{ii} + \sigma_{jj})}\right)^3 \tag{6}$$

A binary interaction parameter, k_{ij_eps}, for correction of the cross-association energy can be also applied, when required, to account for the deviations from the value calculated through the original mixing rule. It is important to highlight that either in the dispersive or association interactions only energy-related binary

parameters were applied in this work since the use of size-related binary parameters is unusual and not recommended [37].

3.2. PC-SAFT pure-component parameter estimation

Ji et al. [38], Nann et al. [39] and Passos et al. [40] reported the use of PC-SAFT to model IL solutions while Zubeir et al. [28] used this EoS to model the CO_2 solubilities in DES with [Ch]Cl, and different symmetrical quaternary ammonium chlorides serving as HBA. The various authors treated ILs as molecules with associative behavior by using a 2B association scheme (according to Huang and Radosz [41]), where to each molecule two association sites (mimicking the cation and the anion) are assigned and association interactions between unlike sites are allowed.

The molecular parameters for $[N_{1111}]Cl$ and $[N_{2222}]Cl$ were directly taken from Ref. [28] and the same approach was here followed to obtain the $[N_{3333}]Cl$ parameters. Thus, the association scheme (2B) and the corresponding association parameters from $[N_{1111}]Cl$ and $[N_{2222}]Cl$ were applied to $[N_{3333}]Cl$. The remaining parameters m_i^{seg}, σ_i, and u_i as well as one temperature-independent binary interaction parameter k_{ij} between water and $[N_{3333}]Cl$ were fitted to experimental water activity coefficients (at 298.15 K, Table S4) and mixtures densities of water + $[N_{3333}]Cl$ solutions (Table S7). The result of the parameter estimation is depicted in Fig. 1, and the PC-SAFT parameters for the quaternary ammonium chlorides and water are summarized in Table 2. It should be noted that $m\sigma^3$ linearly correlates with the molecular weight of the quaternary ammonium salts emphasizing the physical meaning of the size-related parameters. ($m\sigma^3 = 1.2966M_W + 20.749$; $R^2 = 0.9942$; considering $[N_{1111}][Cl]$, $[N_{2222}]Cl$ and $[N_{4444}][Cl]$ from Zubeir et al. [28] and $[N_{3333}][Cl]$ from this work).

The phase behavior of carboxylic acids is complex due to their strong hydrogen-bonding character. Their particular association behavior results in two hydrogen bonds formed simultaneously, which leads to a dimerization in the vapor phase. Kleiner et al. [43] addressed this subject by applying and comparing two different association schemes (1A and 2B) to some carboxylic acids. While the former enables the formation of only dimers, the latter also allows the formation of clusters with more than two acid molecules. The results by Kleiner et al. [43] showed that both association schemes provided good results but using a one-site association scheme yielded an improved description of vapor-pressure data. Nevertheless, this specific thermodynamic feature is more important especially for carboxylic acids of lower molecular weight. In fact, Albers et al. [44] applied the 2B association scheme to model different carboxylic acids achieving a good description of the experimental data by considering that each acid molecule contains two different association sites: an acceptor site at the oxygen atom and a donor site mimicking the hydroxyl group. Thus, the 2B association scheme was applied also for the carboxylic acids studied in this work, and the deviations (%ARD(ρ_L) and %ARD(P^*) in Table 3) were found to be much lower compared to modeling with the 1A association scheme (results not shown in this work).

Thus, the pure-component parameters for lauric acid and myristic acid were inherited from Albers et al. [44], while pure-component parameters for capric acid, palmitic acid and stearic acid were adjusted in the present work by regression to pure fluid liquid-density ρ_L and vapor pressure P^*, data. The results obtained are depicted in Fig. 2 and the parameters reported in Table 3, along with the deviations to the experimental data.

Furthermore, as commonly observed for homologous series, the optimized molecular parameters of SAFT-type equations can be correlated with the compounds molecular weight. This allows predicting pure-component parameters for compounds of different chain length or decreasing the number of parameters to be included in the parameter estimation procedure. Thus, the non-associative pure-component parameters reported in Table 3 were correlated with the molecular weight of the carboxylic acids and linear trends were observed as described by Equations (7)–(9).

$$m_i^{seg} = 0.0044198M_w + 6.3885; R^2 = 0.9808 \quad (7)$$

$$m_i^{seg}\sigma_i^3\left(\text{Å}^3\right) = 1.8145M_w - 46.551; R^2 = 0.9999 \quad (8)$$

$$m_i^{seg}u_i(K) = 3.2523M_w + 1174.7; R^2 = 0.9933 \quad (9)$$

This supports the physical meaning behind the adjusted PC-SAFT parameters. Additionally, the associative parameters can often be set to constant values for components within a homologous series since the associative behavior and interactions in the pure fluid are generally not strongly influenced by the compounds chain length (except for the components with very small chain

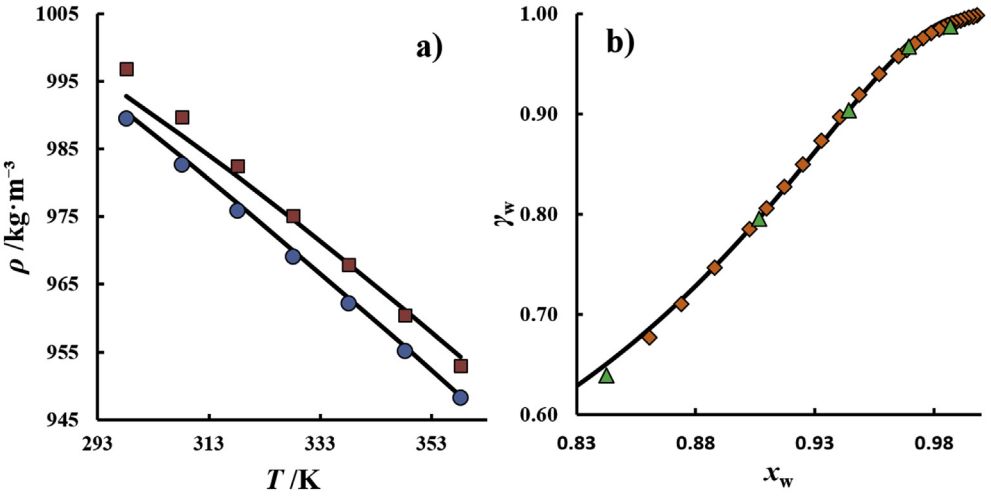

Fig. 1. a) Experimental densities of aqueous solutions of $[N_{3333}]Cl$ measured in this work at atmospheric pressure: ■, $x_{IL} = 0.0931$; ●, $x_{IL} = 0.1608$. b) Water activity coefficients at 298.15 K: ♦, Lindenbaum et al. [42]; ▲, this work. Symbols represent experimental data while the solid lines depict the PC-SAFT results using $k_{ij} = -0.1167$ between water and $[N_{3333}]Cl$.

Table 2
PC-SAFT molecular parameters for symmetrical quaternary ammonium chlorides (2B association scheme).

Salt	$M_w(g/mol)$	m_i^{seg}	σ_i(Å)	$u_i(K)$	$\varepsilon^{AiBi}(K)$	κ^{AiBi}	$\%ARD(\gamma_w)$[a]	$\%ARD(\rho_L)$[a]
$[N_{1111}]Cl$[b]	109.60	6.597	2.9160	451.63	5000	0.1	–	–
$[N_{2222}]Cl$[b]	165.70	17.670	2.3510	278.06	5000	0.1	–	–
$[N_{3333}]Cl$	221.81	17.789	2.6151	217.95	5000	0.1	0.40	0.12
Water[c]	18.02	1.2047	[d]	353.95	2425.67	0.045	–	–

[a] ARD, average relative deviation.
[b] Parameters taken from Zubeir et al. [28].
[c] Parameters taken from Fuchs et al. [72].
[d] Temperature-dependent segment diameter: $\sigma = 2.7927 + 10.11 \cdot \exp(-0.01775 \cdot T\,[K]) - 1.417 \cdot \exp(-0.01146 \cdot T\,[K])$.

Table 3
PC-SAFT pure-component parameters for monocarboxylic acids (2B association scheme).

Acid	$M_w(g/mol)$	m_i^{seg}	σ_i(Å)	$u_i(K)$	$\varepsilon^{AiBi}(K)$	κ^{AiBi}	$\%ARD(\rho_L)$[a]	$\%ARD(P^*)$[a]
Capric	172.26	7.1472	3.3394	242.46	2263.0	0.02	0.96	1.90
Lauric[b]	200.32	7.2547	3.5244	252.97	3047.5	0.00338	0.34 [44]	0.60 [44]
Myristic[b]	228.37	7.4126	3.6719	256.48	2252.5	0.04399	0.57 [44]	0.46 [44]
Palmitic	256.42	7.5599	3.8092	267.52	2291.4	0.02	0.17	1.70
Stearic	284.48	7.6146	3.9536	275.20	2351.6	0.02	0.10	2.20

[a] ARD, average relative deviation.
[b] Parameters taken from Albers et al. [44].

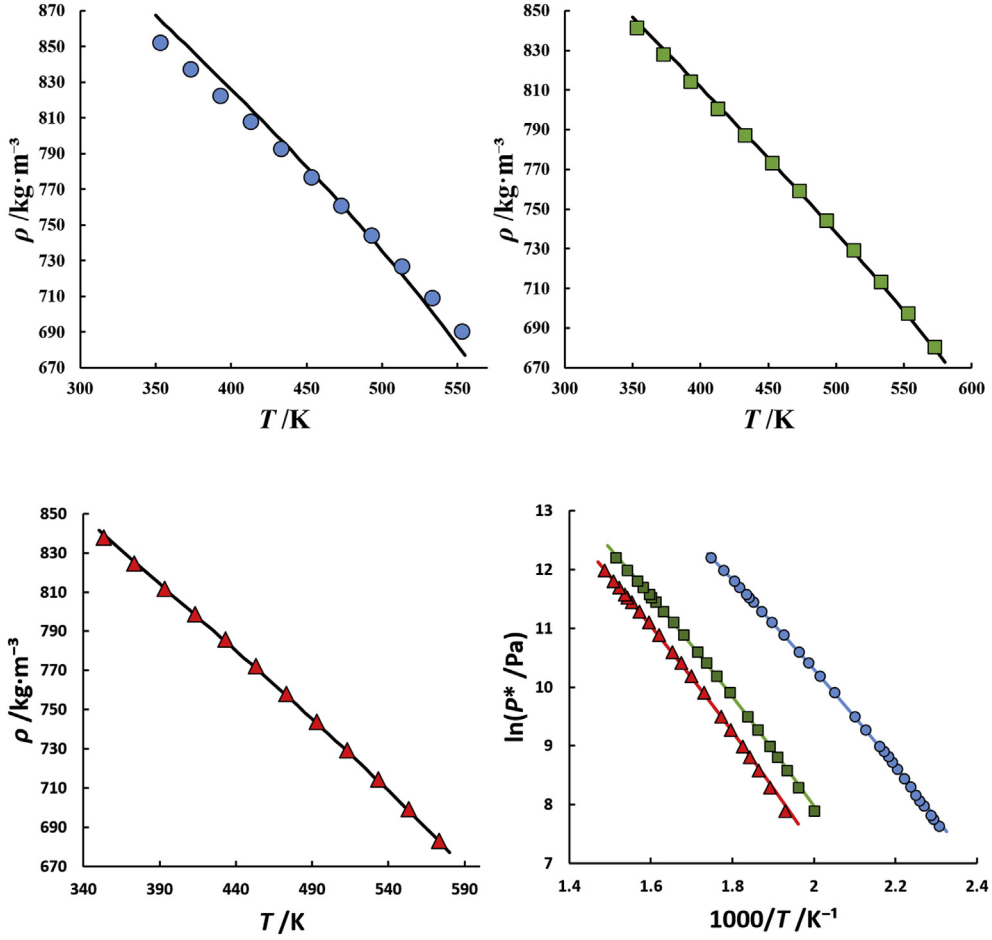

Fig. 2. Densities and vapor pressures of pure monocarboxylic acids. The symbols represent experimental data from Ref. [45] while the solid lines represent the PC-SAFT results for capric acid (●), palmitic acid (■) and stearic acid (▲), respectively.

length). Thus, the association volume was set to a value of 0.02 for palmitic acid, capric acid, and stearic acid, and similar values for the association energy parameter were obtained for these carboxylic acids in the parameter estimation (see Table 3).

3.3. Solid-liquid equilibrium modeling

All the DES constituents considered in this work (quaternary ammonium salts and carboxylic acids) are solids at room temperature. Their solubility in a liquid solvent can be described by a simplified thermodynamic expressions for solid–liquid equilibria according to [46]:

$$x_i^l \gamma_i^l = \exp\left[\left(\frac{\Delta H_i^{sl}}{RT_{mi}}\right)\left(\frac{T - T_{mi}}{T}\right)\right] \quad (10)$$

where x_i^l is the mole fraction of the component i in the liquid phase (solubility), γ_i^l is the activity coefficient of the component i in the liquid phase, T_{mi} and ΔH_i^{sl} are the melting temperature (K) and melting enthalpy ($J \cdot mol^{-1}$) of the pure component i, T is the melting temperature (K) of the mixture, and R is the ideal gas constant (8.314 $J \cdot mol^{-1} \cdot K^{-1}$). This equation considers that pure compounds do not present polymorphic forms, what is acceptable since the solid-solid transition temperature of the fatty acids are very close to the melting temperature, or below the eutectic point [47–49]. Additionally, the effect of the difference between specific heats of the solid and liquid phases was neglected since the heat capacities for fatty acids, and salts, are commonly much lower than their enthalpy values [50–52]. Moreover, Equation (10) assumes that the pure compounds are independently crystallized in the solid phase as expected from a eutectic-type phase diagram. Therefore, the solid phase can be assumed as composed by two pure components without presence of mixed crystals, such that the activity in the solid phase $x_i^s \gamma_i^s = 1$.

An ideal mixture is characterized by activity coefficients in the liquid phase that are equal to one ($\gamma_i^l = 1$). Although clearly non-ideal, the mixtures under investigation were also treated as ideal mixtures in order to evaluate the non-ideality of the compounds in the liquid phase.

The liquidus lines can be obtained through Equation (10) where the activity coefficients need to be considered due to the non-ideality of the studied systems. Applying Equation (10) allows determination of an experimental value for the activity coefficients, which can be used to validate thermodynamic models (in this work PC-SAFT).

Using PC-SAFT, the activity coefficients are calculated from the fugacity coefficients through Equation (11).

$$\gamma_i = \frac{\varphi_i}{\varphi_i^0} \quad (11)$$

where φ_i and φ_i^0 are the fugacity coefficients of component i in the mixture and that of the pure compound, respectively. Fugacity coefficients in the mixture depend on the components, mixture composition, density and temperature, and were derived from the residual Helmholtz energy a^{res} using thermodynamic standard relations.

To evaluate the accuracy of PC-SAFT, the deviations between PC-SAFT modeled melting temperatures T^{calc} and experimental data T^{exp} are expressed in terms of *AAD* (average absolute deviation) applying Equation (12) where N_{exp} is the total number of experimental points in the mixture (excluding the melting points of the pure components):

$$AAD(K) = \frac{1}{N_{exp}} \sum_{k=1}^{N_{exp}} \left| T_k^{calc}(K) - T_k^{exp}(K) \right| \quad (12)$$

4. Results and discussion

Table 4 presents the melting temperatures and enthalpies for the pure compounds studied in this work as well as values from literature. The melting properties of the carboxylic acids under study are in very good agreement with those from literature. Melting temperatures of the quaternary ammonium salts are very scarce in literature, and melting enthalpy data for these compounds was not found in the open literature. The values for the melting points of the three quaternary ammonium salts under study were measured by DSC and confirmed with the melting points measured by the Büchi apparatus. $[N_{1111}]Cl$ decomposed upon heating and it was thus impossible to measure its melting enthalpy, that was fitted to the experimental data for the SLE phase diagrams measured, using the activity coefficients estimated by the COSMO-RS model [53].

Fig. 3 shows the 15 SLE phase diagrams measured in this work. They exhibited a phase behavior characterized by a single eutectic point, with a melting temperature much lower than that of the quaternary ammonium salt used, like commonly found in DES. The detailed melting experimental data obtained for each mixture are reported in supporting information (Tables S1–S3).

Considering the simple eutectic behavior observed for these systems, they were modeled with Equation (10) by two methods: i) considering ideal liquid phase ($\gamma_i = 1$) and ii) as non-ideal liquid phase with activity coefficients calculated with PC-SAFT EoS. The SLE modeling results with activity coefficients obtained from PC-SAFT for the systems under study are illustrated in Fig. 3, while the comparison with the ideal solubility curves is depicted in Fig. 4 for the system $[N_{2222}]Cl$ + lauric acid, and in supporting information for all other systems under study (Figs. S2–S6).

Fig. 3 shows that PC-SAFT is able to provide a good description of the experimental data using either one or two binary parameters (accounting for corrections to the cross-dispersion energy and/or cross-association energy). The binary parameters are listed in Table 5. They were obtained by optimizing an objective function that equaled to a minimization of the AAD(T) given in Equation (12) using all the experimental SLE data listed in Tables S1–S3. Using the pure-component parameters listed in Tables 2 and 3, the melting properties in Table 4 and the binary interaction parameters in Table 5 in order to model the SLE using Equation (10) allows to accurately describe the experimental data. The highly unsymmetrical non-ideal behavior that characterizes these mixtures is correctly described with PC-SAFT. That is, the solubility curves of the quaternary ammonium salts are much more non-ideal than the solubility curves of the carboxylic acids. This is also graphically illustrated in Fig. 4 by the values of the activity coefficients in the system $[N_{2222}]Cl$ + lauric acid: these values are very low (close to zero) for the quaternary ammonium salts whereas values by one order of magnitude higher can be observed for the carboxylic acid.

This highly unsymmetrical non-ideality was observed for all systems under study, and is presented in Figs. S2–S6 of the supporting information. Besides some small quantitative differences between the activity coefficients of the quaternary ammonium salts in the systems under study, a big qualitative difference between the activity coefficients of the carboxylic acids in the DES under study becomes obvious. In the systems containing $[N_{1111}]Cl$, very small deviations to ideality can be found as the activity coefficients of the

Table 4
Melting properties for pure compounds measured in this work and comparison with literature.

Components	T_m/K			$\Delta H^{sl}(kJ/mol)$		
	This work	Literature	Ref.	This work	Literature	Ref.
Quaternary ammonium salts						
$[N_{1111}]Cl$	612.87 ± 6.16	693.15	[54]	20.49	–	–
$[N_{2222}]Cl$	526.78 ± 1.03	–	–	51.24 ± 0.02	–	–
$[N_{3333}]Cl$	503.07 ± 2.56	416.15–418.15	[55]	66.58 ± 2.10	–	–
Fatty acids						
Capric Acid	304.75 ± 0.05	305.48	[56]	27.50 ± 1.29	27.23	[56]
		305.30	[57]		28.00	[57]
		303.80	[58]		28.30	[58]
		304.95	[59]		28.60	[59]
Lauric Acid	317.48 ± 0.14	318.48	[56]	37.83 ± 0.20	34.62	[56]
		316.20	[58]		36.10	[58]
		317.82	[60]		34.69[b]	[60]
		317.45	[61]		36.30	[61]
Myristic Acid	327.03 ± 0.04	328.93	[56]	41.29 ± 0.38	43.95	[56]
		326.50	[58]		45.00	[58]
		326.20	[62]		45.75[b]	[62]
		327.45	[61]		45.20	[61]
Palmitic Acid	336.84 ± 0.10	336.36	[63]	51.02 ± 0.22	53.02	[63]
		337.69	[64]		51.37	[64]
		335.44	[65]		55.85	[65]
		335.40	[66]		53.90	[66]
Stearic Acid	343.67 ± 0.07	344.04	[63]	61.36 ± 0.42	61.10	[63]
		343.65	[67]		59.96	[67]
		343.85	[68]		59.96	[68]
		342.75	[69]		61.30	[69]

carboxylic acids are close to one, and usually values $\gamma^L_{acid} > 1.0$) were observed. However, upon increasing the chain length of the alkyl groups of the quaternary ammonium salt, negative deviations to ideality were also observed based on the fact that the values $\gamma^L_{acid} << 1.0$. That is, the attractive interactions strongly increase with increasing chain length of the quaternary ammonium salt, and a moderate increase can also be observed with increasing chain length of carboxylic acid. This behavior suggests a strengthening of the HBA:HBD complex due to the weakening of the coulombic interactions between the cation and anion of the salt with the increase of its alkyl chains, which has been described by Kurnia et al. [70] for the interactions of ionic liquids and water through hydrogen bonding.

In general, extreme strong negative deviations from ideal mixture behavior is found in all DES under study causing a large decrease in the system melting temperature. Strong associative interactions (hydrogen bonding) between the two DES constituents are the main reason for the observed negative deviations to ideality. Cross-association occurs between the carboxylic acid that acts as H-bonding donor and the quaternary ammonium salt that acts as H-bonding acceptor. These strong cross interactions explain very low activity coefficients. However, activity coefficients of the carboxylic acids are larger than one at very high concentration of carboxylic acid in the mixture. In these concentration regions, self-association interactions between the carboxyl groups become stronger than in the pure-component state, and cross-association interactions play a minor role [48,57]. Thus, the melting-point depressions are higher the higher the amount of quaternary ammonium salt present in the mixture. This explains the behavior of the almost horizontal liquidus line of carboxylic acid shown in Fig. 3. In fact, the eutectic behavior observed in these systems is not trivial, as the complex interaction behavior is additionally confronted by very large differences between the melting temperatures of the DES constituents. This prevents high melting-point depressions in regions with high concentration of carboxylic acid, which forces the eutectic temperature close to the melting temperature of the pure carboxylic acid [71] (note in Figs. S2–S6 that the ideal solubility curves exhibit this behavior).

In contrast to the close-to-ideal phase behavior at high concentrations of carboxylic acids, negative deviations to ideality are very high at higher concentrations of quaternary ammonium salt. The deviations to the experimental data (in terms of AAD (in K)) applying Equation (10) under the assumption of ideal mixture behavior is depicted in Fig. 5. High deviations to the experimental data can be observed due to the significant negative deviations from ideal behavior at high concentrations of quaternary ammonium salt. Thus, advanced thermodynamic models such as PC-SAFT are required in order to quantify activity coefficients and to improve the accuracy of Equation (10). PC-SAFT allows for a good description of most systems with a global AAD (K) of only 7.39 K for all the systems studied in this work. Taking into account the large temperature range studied (about 300 K), these results can be considered as a very satisfactory result.

One drawback of the measurements is the time they consume. A huge number of measurements is required in order to quantify the eutectic point (eutectic temperature T^E and composition x^E), allowing also to assess the temperature difference between ideal T^E and real T^E (assigned with ΔT^E). To overcome this time limitation, PC-SAFT was applied in this work in order to estimate the eutectic point of the DES under study. For that purpose, the pure-component parameters in Tables 2 and 3 and the binary parameters in Table 5 were used. The modeling results are depicted in Fig 6. Fig. 6 suggests that the eutectic composition is shifted towards lower mole fractions of acid upon increasing alkyl chain of both, the acid and the quaternary ammonium salt. In spite of the uncertainties of experimental data and PC-SAFT modeling associated to these estimates it can be stated that a fixed stoichiometric relationship between carboxylic acid and quaternary ammonium

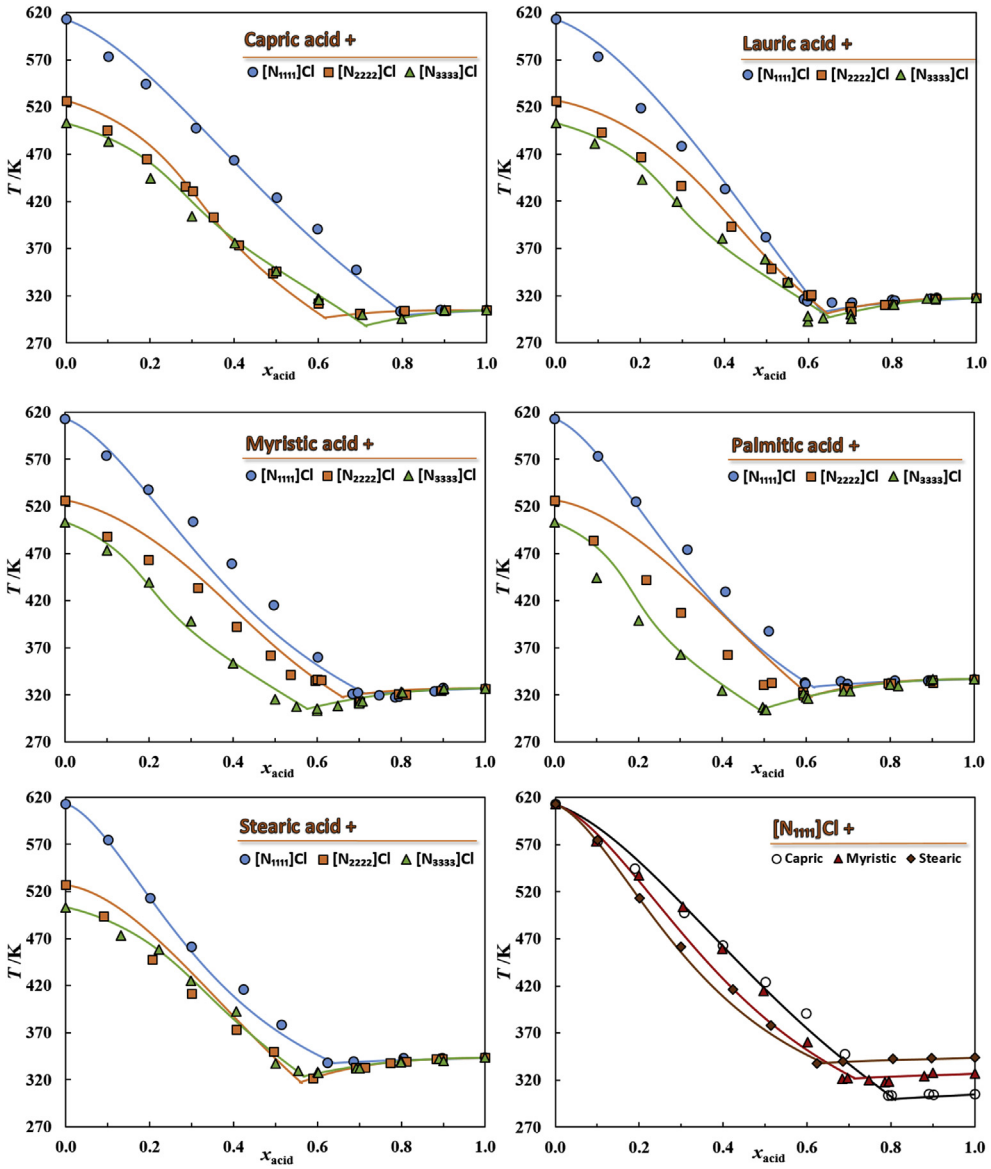

Fig. 3. Solid-liquid phase diagrams of DES composed of monocarboxylic acids and symmetrical quaternary ammonium chlorides. Symbols represent the experimental data measured in this work while the solid lines depict the PC-SAFT modeling.

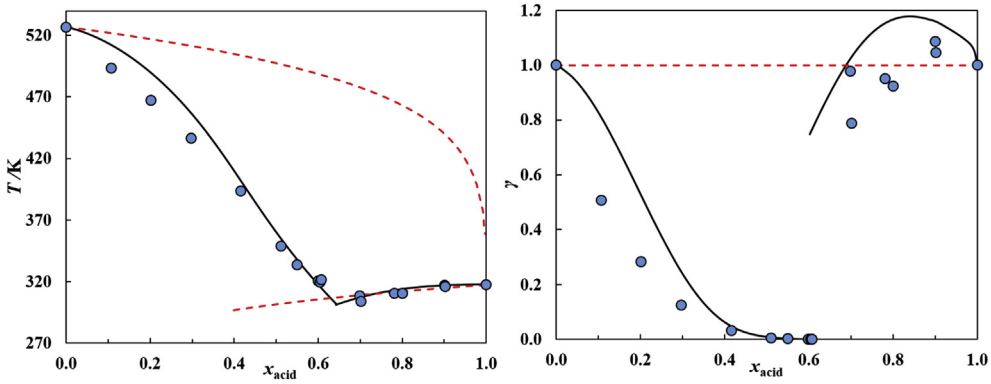

Fig. 4. Solid-liquid equilibrium (left) and activity coefficients (right) for the DES $[N_{2222}]Cl$ + lauric acid. Legend: ●, experimental; —,PC-SAFT; ---, ideal.

Table 5
Binary parameters applied within PC-SAFT model.

Systems	PC-SAFT binary parameters	
	k_{ij}	k_{ij_eps}
$[N_{1111}]Cl$ + capric acid	−0.178	–
$[N_{1111}]Cl$ + lauric acid	−0.210	–
$[N_{1111}]Cl$ + myristic acid	−0.220	–
$[N_{1111}]Cl$ + palmitic acid	−0.220	–
$[N_{1111}]Cl$ + stearic acid	−0.220	–
$[N_{2222}]Cl$ + capric acid	−0.085	−0.270
$[N_{2222}]Cl$ + lauric acid	−0.100	−0.180
$[N_{2222}]Cl$ + myristic acid	−0.120	−0.140
$[N_{2222}]Cl$ + palmitic acid	−0.140	−0.096
$[N_{2222}]Cl$ + stearic acid	−0.160	−0.060
$[N_{3333}]Cl$ + capric acid	−0.050	−0.280
$[N_{3333}]Cl$ + lauric acid	−0.050	−0.250
$[N_{3333}]Cl$ + myristic acid	−0.050	−0.290
$[N_{3333}]Cl$ + palmitic acid	−0.050	−0.320
$[N_{3333}]Cl$ + stearic acid	−0.050	−0.220

salt is not observed. This is not surprising as the systems under study do not obey co-crystal formation with a fixed stoichiometric composition. It is possible however to state that the liquid mixture seems to be dominated by associates with molar ratios of 2:1 for the considered DES carboxylic acid/quaternary ammonium salt.

The eutectic temperature increases with increasing chain length of the carboxylic acid. This is expected as the pure-acid melting temperature limits the eutectic temperature of the system, i.e. the lower the melting temperature for the pure acid, the lower T^E values. Further, it can be observed from Fig. 6 that T^E decreases from $[N_{1111}]Cl$ to $[N_{3333}]Cl$, which can be explained by the decrease of melting points of the quaternary ammonium salts from $[N_{1111}]Cl$ to $[N_{3333}]Cl$ combined with the increased non-ideality of the liquid phase from $[N_{1111}]Cl$ to $[N_{3333}]Cl$ (see supporting information).

Concerning the temperature difference ΔT^E (i.e. the difference between the eutectic temperature estimated by PC-SAFT and that calculated considering an ideal liquid phase for the estimated eutectic composition), an increase following the order: $[N_{1111}]Cl > [N_{2222}]Cl > [N_{3333}]Cl$ can be observed from Fig. 6, which is mainly due to the melting temperatures of the pure quaternary ammonium salts. In contrast, activity coefficients of the salts decrease in the order $[N_{1111}]Cl > [N_{2222}]Cl > [N_{3333}]Cl$, as illustrated in Figs. S3–S6. Thus, the strength of cross interactions increase in the order $[N_{1111}]Cl < [N_{2222}]Cl < [N_{3333}]Cl$ between the salt and the carboxylic acid. The very large temperature difference observed are a strong evidence that the systems studied here are, in fact, deep eutectic mixtures.

These observations are further reinforced by the binary parameters estimated for quantitative PC-SAFT modeling. As already known, one of the advantages of using these coarse-grained models is the enhanced physical meaning of the model parameters, when compared to activity coefficients models. The binary k_{ij_eps} accounts for deviations in the cross-association energy obtained through the conventional mixing rules. The fact that k_{ij_eps} takes negative values confirms the strong cross-association between acid and salt in the considered DES. According to Table 5, the k_{ij_eps} values become more negative in the order $[N_{1111}]Cl < [N_{2222}]Cl < [N_{3333}]Cl$, supporting the interpretation for an increase of the cross-association strength in that order.

Despite the importance of hydrogen bonding, also dispersion forces are important in the DES under study. In order to quantitatively model the phase diagrams shown in Figs. 3–4, one binary interaction parameter k_{ij} that accounts for deviations to the mixture's dispersive energy was applied to each mixture. According to

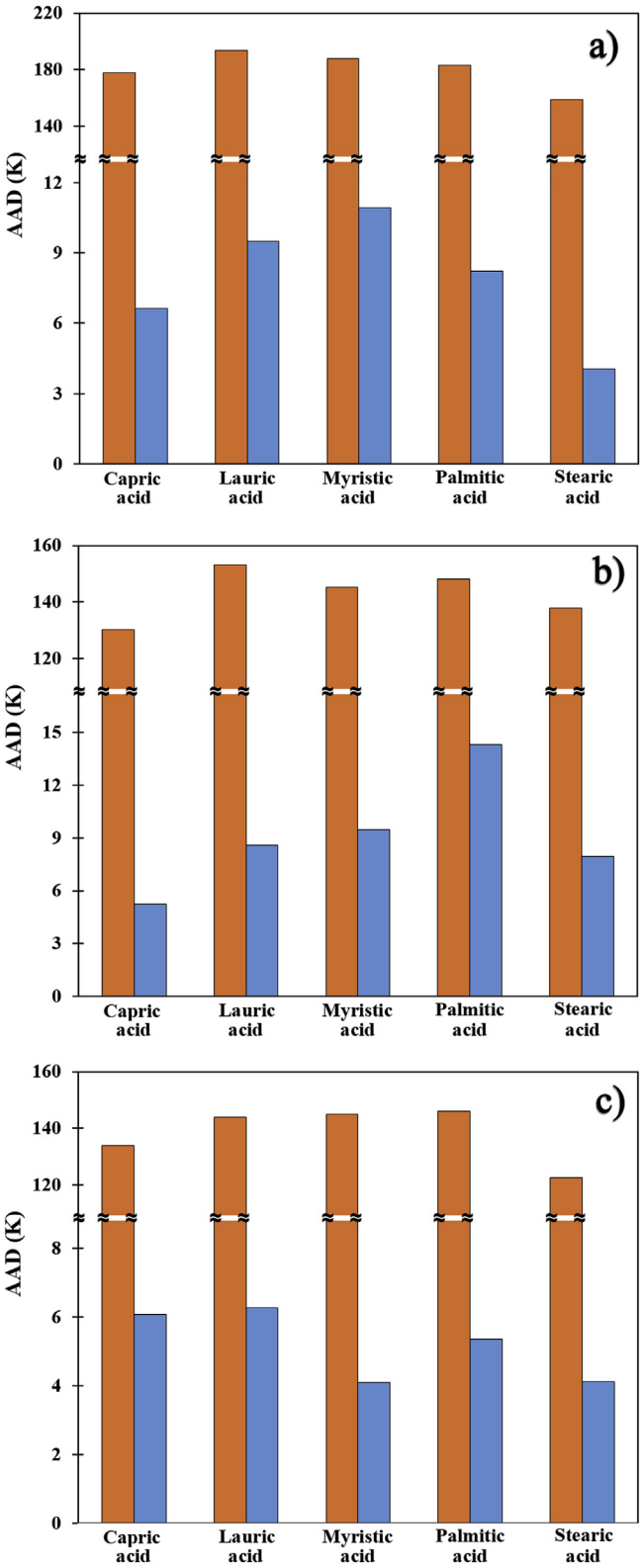

Fig. 5. Deviations to the experimental data measured in this work: ■, ideal; ■, PC-SAFT for a) $[N_{1111}]Cl$ + carboxylic acids b) $[N_{2222}]Cl$ + carboxylic acids c) $[N_{3333}]Cl$ + carboxylic acids.

Table 5, the values obtained were also negative, which means an increased mixture's dispersive energy compared to the ideal combining rule and points to very strong cross-dispersion

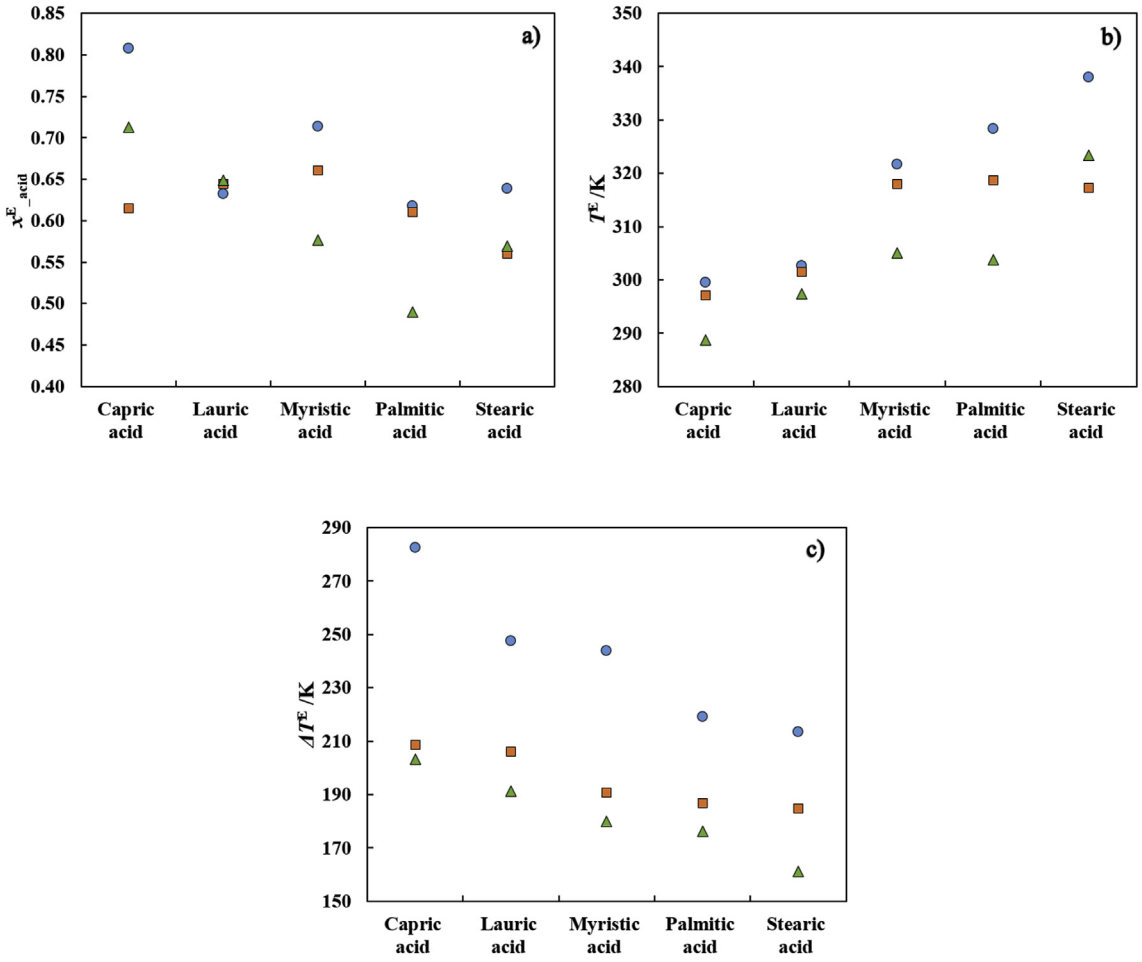

Fig. 6. a) Eutectic compositions b) eutectic temperatures c) temperature difference of the various DES studied, estimated by PC-SAFT. ●, $[N_{1111}]Cl$; ■, $[N_{2222}]Cl$; ▲, $[N_{3333}]Cl$.

interactions. As often observed for a series of mixtures with mixing partner from one family (e.g. water-alkane, gas-alkane and many more), the parameter k_{ij} can be correlated with molecular weight of the mixing partner. In the DES studied in this work, k_{ij} values become more negative upon increasing the alkyl chain length of the carboxylic acid. In Table 5, an exception can be found for the DES with $[N_{3333}]Cl$, where k_{ij} values were applied that were independent of the chain length of the carboxylic acid. For these mixtures, cross-association interactions obviously dominate the physical behavior of the mixtures, and dispersion interactions are less important compared to the DES with $[N_{1111}]Cl$ or $[N_{2222}]Cl$. It should be noted that a linear dependence of k_{ij_eps} on the molecular weight of the carboxylic acids could have been obtained, if the dispersive energy binary parameter k_{ij} had been assumed to be set as individual values for each ammonium salt/carboxyclic acid. This was not desired and thus avoided in this work.

In sum, the binary parameters applied were found to follow these dependencies on molecular weight of the carboxylic acid:

$$k_{ij}(N_{1111}Cl) = 6.715 \times 10^{-6} \times M^2_{w\_acid} - 3.402 \times 10^{-3} \times M_{w\_acid} + 0.2066\left(R^2 = 0.9634\right) \quad (13)$$

$$k_{ij}(N_{2222}Cl) = -6.773 \times 10^{-4} \times M_{w\_acid} + 0.03367\left(R^2 = 0.9972\right) \quad (14)$$

$$k_{ij}(N_{3333}Cl) = -0.05 \quad (15)$$

$$k_{ij\_eps}(N_{2222}Cl) = 0.4063 \times ln(M_{w\_acid}) - 2.350\left(R^2 = 0.9823\right) \quad (16)$$

These correlations allow predicting interaction parameters for mixtures that are not presented in this work, or alternatively to decrease the number of required binary parameters, reducing considerably the amount of experimental data to be gathered in order to correctly describe the SLE behavior of this type of DES.

5. Conclusions

(Solid+liquid) phase equilibrium diagrams for 15 different DES composed of carboxylic acids and symmetrical quaternary ammonium chlorides were measured by a combination of DSC and visual methods. The experimental data obtained showed that these systems present a single-eutectic type behavior, with a eutectic temperature very close to the melting temperature of pure carboxylic acid, and a very large negative deviation from ideal-mixture

behavior, that becomes more pronounced as the chain length of the quaternary ammonium salt increases. This behavior suggests a strengthening of the HBA:HBD complex upon weakening the coulombic interactions between the cation and anion of the salt with the increase of its alkyl chain length.

The modeling of the studied systems was performed applying the molecular-based PC-SAFT EoS. The pure-component PC-SAFT parameters were either taken from literature, or fitted to experimental data of the pure compound for the acids, or, in the case of the salts, to activity data and density data of their aqueous solutions. By using one or two binary parameters (that in most cases can be kept constant or correlated to the molecular weight of the fatty acid), a good quantitative description (an average AAD of only 7.39 K) of the experimental data was achieved, despite the complex cross-association and large asymmetry of the studied mixtures. PC-SAFT modeling allowed to estimate the eutectic points of the DES under study. The physical meaning of the parameters within this model was also enhanced and insights into the molecular interactions in the systems were given. In more detail, the binary parameters accounting for deviations in the cross-association energy and cross-dispersion energy suggested the increase in cross-association (cross-dispersion) as the number of CH_2 groups in the salt (acid) increased.

The results here reported show that PC-SAFT can be a valuable tool in the description of the SLE of DES, and allows for a better understanding of phase behavior and interactions within this type of deep eutectic mixtures.

Acknowledgements

This work was developed in the scope of the project CICECO – Aveiro Institute of Materials, POCI-01-0145-FEDER-007679 (Ref. FCT UID/CTM/50011/2013) and LSRE-LCM, POCI-01-0145-FEDER-006984|UID/EQU/50020/2013, financed by national funds through the FCT/MEC and when appropriate co-financed by FEDER under the PT2020 Partnership Agreement. M.A.R.M acknowledges FCT for her PhD grant (SFRH/BD/87084/2012). FCT is also acknowledged for funding the project DeepBiorefinery (PTDC/AGR-TEC/1191/2014). P.V.A.P., G.J.M., M.D.H. and E.A.C.B thank the national funding agencies CNPq (National Council for Scientific and Technological Development) (305870/2014-9, 309780/2014, 406856/2013-3), FAPESP (Research Support Foundation of the State of São Paulo) (2014/21252-0, 2016/08566-1), FAEPEX/UNICAMP (Fund for Research, Teaching, and Extension) (0125/16) and CAPES (Coordination of Improvement of Higher Level Personnel) for financial support and scholarships. E.A.C thanks Erasmus+ program of the European Union for co-funding.

Appendix A. Supplementary data

Supplementary data related to this article can be found at http://dx.doi.org/10.1016/j.fluid.2017.04.007.

References

[1] A.P. Abbott, G. Capper, D.L. Davies, R.K. Rasheed, V. Tambyrajah, Novel solvent properties of choline chloride/urea mixtures, Chem. Commun. 99 (2003) 70–71, http://dx.doi.org/10.1039/b210714g.
[2] Q. Zhang, K. De Oliveira Vigier, S. Royer, F. Jérôme, Deep eutectic solvents: syntheses, properties and applications, Chem. Soc. Rev. 41 (2012) 7108–7146, http://dx.doi.org/10.1039/c2cs35178a.
[3] E.L. Smith, A.P. Abbott, K.S. Ryder, Deep eutectic solvents (DESs) and their applications, Chem. Rev. 114 (2014) 11060–11082, http://dx.doi.org/10.1021/cr300162p.
[4] B. Tang, K.H. Row, Recent developments in deep eutectic solvents in chemical sciences, Monatsh. Für Chem. - Chem. Mon. 144 (2013) 1427–1454, http://dx.doi.org/10.1007/s00706-013-1050-3.
[5] M. Francisco, A. van den Bruinhorst, M.C. Kroon, Low-transition-temperature mixtures (LTTMs): a new generation of designer solvents, Angew. Chem. Int. Ed. 52 (2013) 3074–3085, http://dx.doi.org/10.1002/anie.201207548.
[6] Z. Maugeri, P. Domínguez de María, Novel choline-chloride-based deep-eutectic-solvents with renewable hydrogen bond donors: levulinic acid and sugar-based polyols, RSC Adv. 2 (2012) 421–425, http://dx.doi.org/10.1039/C1RA00630D.
[7] A. Hayyan, F.S. Mjalli, I.M. Alnashef, Y.M. Al-Wahaibi, T. Al-Wahaibi, M.A. Hashim, Glucose-based deep eutectic solvents: physical properties, J. Mol. Liq. 178 (2013) 137–141, http://dx.doi.org/10.1016/j.molliq.2012.11.025.
[8] C. Ruß, B. König, Low melting mixtures in organic synthesis – an alternative to ionic liquids? Green Chem. 14 (2012) 2969–2982, http://dx.doi.org/10.1039/c2gc36005e.
[9] P.M. Pawar, K.J. Jarag, G.S. Shankarling, Environmentally benign and energy efficient methodology for condensation: an interesting facet to the classical Perkin reaction, Green Chem. 13 (2011) 2130–2134, http://dx.doi.org/10.1039/C0GC00712A.
[10] N. Azizi, E. Batebi, S. Bagherpour, H. Ghafuri, Natural deep eutectic salt promoted regioselective reduction of epoxides and carbonyl compounds, RSC Adv. 2 (2012) 2289–2293, http://dx.doi.org/10.1039/C2RA01280D.
[11] S.B. Phadtare, G.S. Shankarling, Halogenation reactions in biodegradable solvent: efficient bromination of substituted 1-aminoanthra-9,10-quinone in deep eutectic solvent (choline chloride : urea), Green Chem. 12 (2010) 458–462, http://dx.doi.org/10.1039/B923589B.
[12] A.P. Abbott, G. Capper, D.L. Davies, R.K. Rasheed, P. Shikotra, Selective extraction of metals from mixed oxide matrixes using choline-based ionic liquids, Inorg. Chem. 44 (2005) 6497–6499, http://dx.doi.org/10.1021/ic0505450.
[13] A. Biswas, R.L. Shogren, D.G. Stevenson, J.L. Willett, P.K. Bhowmik, Ionic liquids as solvents for biopolymers: acylation of starch and zein protein, Carbohydr. Polym. 66 (2006) 546–550, http://dx.doi.org/10.1016/j.carbpol.2006.04.005.
[14] G. Garcia, S. Aparicio, R. Ullah, M. Atilhan, Deep eutectic solvents: physicochemical properties and gas separation applications, Energy Fuel 29 (2015) 2616–2644, http://dx.doi.org/10.1021/ef5028873.
[15] H. Zhao, G.A. Baker, Ionic liquids and deep eutectic solvents for biodiesel synthesis: a review, J. Chem. Technol. Biotechnol. 88 (2013) 3–12, http://dx.doi.org/10.1002/jctb.3935.
[16] F.S. Oliveira, A.B. Pereiro, L.P.N. Rebelo, I.M. Marrucho, Deep eutectic solvents as extraction media for azeotropic mixtures, Green Chem. 15 (2013) 1326–1330, http://dx.doi.org/10.1039/C3GC37030E.
[17] F. Pena-Pereira, J. Namieśnik, Ionic liquids and deep eutectic mixtures: sustainable solvents for extraction processes, ChemSusChem 7 (2014) 1784–1800, http://dx.doi.org/10.1002/cssc.201301192.
[18] H.G. Morrison, C.C. Sun, S. Neervannan, Characterization of thermal behavior of deep eutectic solvents and their potential as drug solubilization vehicles, Int. J. Pharm. 378 (2009) 136–139, http://dx.doi.org/10.1016/j.ijpharm.2009.05.039.
[19] H.-G. Liao, Y.-X. Jiang, Z.-Y. Zhou, S.-P. Chen, S.-G. Sun, Shape-controlled synthesis of gold nanoparticles in deep eutectic solvents for studies of structure-functionality relationships in electrocatalysis, Angew. Chem. Int. Ed. Engl. 47 (2008) 9100–9103, http://dx.doi.org/10.1002/anie.200803202.
[20] D. Carriazo, M.C. Serrano, M.C. Gutiérrez, M.L. Ferrer, F. del Monte, Deep-eutectic solvents playing multiple roles in the synthesis of polymers and related materials, Chem. Soc. Rev. 41 (2012) 4996–5014, http://dx.doi.org/10.1039/c2cs15353j.
[21] A.A.C. Toledo Hijo, G.J. Maximo, M.C. Costa, E.A.C. Batista, A.J.A. Meirelles, Applications of ionic liquids in the food and bioproducts industries, ACS Sustain. Chem. Eng. 4 (2016) 5347–5369, http://dx.doi.org/10.1021/acssuschemeng.6b00560.
[22] W.G. Chapman, G. Jackson, K.E. Gubbins, Phase equilibria of associating fluids Chain molecules with multiple bonding sites, Mol. Phys. 65 (1988) 1057–1079, http://dx.doi.org/10.1207/s15327752jpa8502.
[23] W.G. Chapman, K.E. Gubbins, G. Jackson, M. Radosz, New reference equation of state for associating liquids, Ind. Eng. Chem. Res. 29 (1990) 1709–1721, http://dx.doi.org/10.1021/ie00104a021.
[24] E.A. Müller, K.E. Gubbins, Molecular-based equations of state for associating fluids: a review of SAFT and related approaches, Ind. Eng. Chem. Res. 40 (2001) 2193–2211, http://dx.doi.org/10.1021/ie000773w.
[25] P. Paricaud, A. Galindo, G. Jackson, Recent advances in the use of the SAFT approach in describing electrolytes, interfaces, liquid crystals and polymers, Fluid Phase Equilib. 194 (2002) 87–96, http://dx.doi.org/10.1016/S0378-3812(01)00659-8.
[26] J. Gross, G. Sadowski, Perturbed-chain SAFT: an equation of state based on a perturbation theory for chain molecules, Ind. Eng. Chem. Res. 40 (2001) 1244–1260, http://dx.doi.org/10.1021/ie0003887.
[27] S.P. Verevkin, A.Y. Sazonova, A.K. Frolkova, D.H. Zaitsau, I.V. Prikhodko, C. Held, Separation performance of BioRenewable deep eutectic solvents, Ind. Eng. Chem. Res. 54 (2015) 3498–3504, http://dx.doi.org/10.1021/acs.iecr.5b00357.
[28] L.F. Zubeir, C. Held, G. Sadowski, M.C. Kroon, PC-SAFT modeling of CO2 solubilities in deep eutectic solvents, J. Phys. Chem. B 120 (2016) 2300–2310, http://dx.doi.org/10.1021/acs.jpcb.5b07888.
[29] W.J. Hamer, Y. Wu, Osmotic coefficients and mean activity coefficients of uni-univalent electrolytes in water at 25°C, J. Phys. Chem. Ref. Data 1 (1972) 1047–1100, http://dx.doi.org/10.1063/1.3253108.

[30] D.G. Archer, Thermodynamic properties of the NaBr+H2O system, J. Phys. Chem. Ref. Data 20 (1991) 509–555, http://dx.doi.org/10.1063/1.555888.
[31] M.S. Wertheim, Fluids with highly directional attractive forces. I. Statistical thermodynamics, J. Stat. Phys. 35 (1984) 19–34, http://dx.doi.org/10.1007/BF01017362.
[32] M.S. Wertheim, Fluids with highly directional attractive forces. II. Thermodynamic perturbation theory and integral equations, J. Stat. Phys. 35 (1984) 35–47, http://dx.doi.org/10.1007/BF01017363.
[33] M.S. Wertheim, Fluids with highly directional attractive forces. III. Multiple attraction sites, J. Stat. Phys. 42 (1986) 459–476, http://dx.doi.org/10.1007/BF01127721.
[34] M.S. Wertheim, Fluids with highly directional attractive forces. IV. Equilibrium polymerization, J. Stat. Phys. 42 (1986) 477–492, http://dx.doi.org/10.1007/BF01127722.
[35] J. Gross, G. Sadowski, Application of the perturbed-chain SAFT equation of state to associating systems application of the perturbed-chain SAFT equation of state to, Ind. Eng. Chem. Res. 41 (2002) 5510–5515, http://dx.doi.org/10.1021/ie010954d.
[36] J.P. Wolbach, S.I. Sandler, Using molecular orbital calculations to describe the phase behavior of cross-associating mixtures, Ind. Eng. Chem. Res. 37 (1998) 2917–2928, http://dx.doi.org/10.1021/ie970781l.
[37] C. Held, A. Prinz, V. Wallmeyer, G. Sadowski, Measuring and modeling alcohol/salt systems, Chem. Eng. Sci. 68 (2012) 328–339, http://dx.doi.org/10.1016/j.ces.2011.09.040.
[38] X. Ji, C. Held, G. Sadowski, Modeling imidazolium-based ionic liquids with ePC-SAFT, Fluid Phase Equilib. 335 (2012) 64–73. http://dx.doi.org/10.1016/j.fluid.2012.05.029.
[39] A. Nann, C. Held, G. Sadowski, Liquid – liquid equilibria of 1 - butanol/water/IL systems, Ind. Eng. Chem. Res. 52 (2013) 18472–18481, http://dx.doi.org/10.1021/ie403246e.
[40] H. Passos, I. Khan, F. Mutelet, M.B. Oliveira, P.J. Carvalho, L.M.N.B.F. Santos, C. Held, G. Sadowski, M.G. Freire, J.A.P. Coutinho, Vapor-liquid equilibria of water plus alkylimidazolium-based ionic liquids: measurements and perturbed-chain statistical associating fluid theory modeling, Ind. Eng. Chem. Res. 53 (2014) 3737–3748, http://dx.doi.org/10.1021/ie4041093.
[41] S.H. Huang, M. Radosz, Equation of state for small, large, polydisperse and associating molecules, Ind. Eng. Chem. Res. 29 (1990) 2284–2294, http://dx.doi.org/10.1021/ie00107a014.
[42] S. Lindenbaum, G.E. Boyd, Osmotic and axtivity coefficients for the symmetrical tetraalkyl ammonium halides in aqueous solution at 25°, J. Phys. Chem. 68 (1964) 911–917, http://dx.doi.org/10.1021/j100786a038.
[43] M. Kleiner, Thermodynamic Modeling of Complex Systems: Polar and Associating Fluids and Mixtures, Department of Biological and Chemical Engineering, Technische Universität Dortmund, 2008. PhD Thesis.
[44] K. Albers, M. Heilig, G. Sadowski, Reducing the amount of PCP–SAFT fitting parameters. 2. Associating components, Fluid Phase Equilib. 326 (2012) 31–44, http://dx.doi.org/10.1016/j.fluid.2012.04.014.
[45] T.E. Daubert, H.M. Sibul, C.C. Stebbins, R.P. Danner, R.L. Rowley, M.E. Adams, W.V. Wilding, T.L. Marshall, Physical and Thermodynamic Properties of Pure Chemicals: DIPPR: Data Compilation: Core + Supplements 1-10, Taylor & Francis, 2000.
[46] J.M. Prausnitz, R.N. Lichtenthaler, E.G. Azevedo, Molecular Thermodynamics of Fluid-phase Equilibria, third ed., Prentice Hall, New Jersey, 1999.
[47] B. Journal, G.J. Maximo, M.C. Costa, A.J.A. Meirelles, Solid-liquid equilibrium of triolein with fatty alcohols, Braz. J. Chem. Eng. 30 (2013) 33–43, http://dx.doi.org/10.1590/S0104-66322013000100005.
[48] G.J. Maximo, N.D.D. Carareto, M.C. Costa, A.O. dos Santos, L.P. Cardoso, M.A. Krähenbühl, A.J.A. Meirelles, On the solid-liquid equilibrium of binary mixtures of fatty alcohols and fatty acids, Fluid Phase Equilib. 366 (2014) 88–98, http://dx.doi.org/10.1016/j.fluid.2014.01.004.
[49] M.C. Costa, M. Sardo, M.P. Rolemberg, P. Ribeiro-Claro, A.J.A. Meirelles, J.A.P. Coutinho, M.A. Krähenbühl, The solid-liquid phase diagrams of binary mixtures of consecutive, even saturated fatty acids: differing by four carbon atoms, Chem. Phys. Lipids 157 (2009) 40–50, http://dx.doi.org/10.1016/j.chemphyslip.2008.09.006.
[50] R.L. Gardas, J.A.P. Coutinho, A group contribution method for viscosity estimation of ionic liquids, Fluid Phase Equilib. 266 (2008) 195–201. http://dx.doi.org/10.1016/j.fluid.2008.01.021.
[51] A. Diedrichs, J. Gmehling, Measurement of heat capacities of ionic liquids by differential scanning calorimetry, Fluid Phase Equilib. 244 (2006) 68–77, http://dx.doi.org/10.1016/j.fluid.2006.03.015.
[52] H. Niedermeyer, J.P. Hallett, I.J. Villar-Garcia, P.A. Hunt, T. Welton, Mixtures of ionic liquids, Chem. Soc. Rev. 41 (2012) 7780–7802, http://dx.doi.org/10.1039/c2cs35177c.
[53] M.A.R. Martins, Studies for the Development of New Separation Processes with Terpenes and Their Environmental Distribution, PhD Thesis, University of Aveiro, 2017.
[54] R.C. Weast (Ed.), Handbook of Chemistry and Physics, 63 Rd, CRC Press, Boca Raton, 1982.
[55] H. Nakayama, Solid-liquid and liquid-liquid phase equilibria in the symmetrical tetraalkylammonium halide–water systems, Bull. Chem. Soc. Jpn. 54 (1981) 3717–3722, http://dx.doi.org/10.1246/bcsj.54.3717.
[56] F.C. de Matos, M.C. da Costa, A.J. de Almeida Meirelles, E.A.C. Batista, Binary solid–liquid equilibrium systems containing fatty acids, fatty alcohols and triolein by differential scanning calorimetry, Fluid Phase Equilib. 404 (2015) 1–8, http://dx.doi.org/10.1016/j.fluid.2015.06.015.
[57] N.D.D. Carareto, T. Castagnaro, M.C. Costa, A.J.A. Meirelles, The binary (solid-+liquid) phase diagrams of (caprylic or capric acid)+(1-octanol or 1-decanol), J. Chem. Thermodyn. 78 (2014) 99–108, http://dx.doi.org/10.1016/j.jct.2014.06.011.
[58] E. Moreno, R. Cordobilla, T. Calvet, M.A. Cuevas-Diarte, G. Gbabode, P. Negrier, D. Mondieig, H.A.J. Oonk, Polymorphism of even saturated carboxylic acids from n-decanoic to n-eicosanoic acid, New J. Chem. 31 (2007) 947–957, http://dx.doi.org/10.1039/b700551b.
[59] T. Inoue, Y. Hisatsugu, M. Suzuki, Z. Wang, L. Zheng, Solid-liquid phase behavior of binary fatty acid mixtures: 3. Mixtures of oleic acid with capric acid (decanoic acid) and caprylic acid (octanoic acid), Chem. Phys. Lipids 132 (2004) 225–234, http://dx.doi.org/10.1016/j.chemphyslip.2004.07.004.
[60] A.K. Misra, M. Misra, G.M. Panpalia, A.K. Dorle, Thermoanalytical and microscopic investigation of interaction between paracetamol and fatty acid crystals, J. Macromol. Sci. Part A 44 (2007) 685–690, http://dx.doi.org/10.1080/10601320701351177.
[61] T. Inoue, Y. Hisatsugu, R. Ishikawa, M. Suzuki, Solid – liquid phase behavior of binary fatty acid mixtures 2. Mixtures of oleic acid with lauric acid, myristic acid, and palmitic acid, Chem. Phys. Lipids 127 (2004) 161–173, http://dx.doi.org/10.1016/j.chemphyslip.2003.10.013.
[62] J. Hong, D. Hua, X. Wang, H. Wang, J. Li, Solid-liquid-gas equilibrium of the ternaries ibuprofen + myristic acid + CO2 and ibuprofen + tripalmitin + CO2, J. Chem. Eng. Data 55 (2010) 297–302, http://dx.doi.org/10.1021/je900342a.
[63] F.C. de Matos, M.C. da Costa, A.J. de A. Meirelles, E.A.C. Batista, Binary solid–liquid equilibrium systems containing fatty acids, fatty alcohols and trilaurin by differential scanning calorimetry, Fluid Phase Equilib. 423 (2016) 74–83, http://dx.doi.org/10.1016/j.fluid.2016.04.008.
[64] J.L. Zeng, Z. Cao, D.W. Yang, F. Xu, L.X. Sun, L. Zhang, X.F. Zhang, Phase diagram of palmitic acid-tetradecanol mixtures obtained by DSC experiments, J. Therm. Anal. Calorim. 95 (2009) 501–505, http://dx.doi.org/10.1007/s10973-008-9274-x.
[65] M.C. Costa, M.P. Rolemberg, A.J.A. Meirelles, J.A.P. Coutinho, M.A. Krähenbühl, The solid–liquid phase diagrams of binary mixtures of even saturated fatty acids differing by six carbon atoms, Thermochim. Acta 496 (2009) 30–37, http://dx.doi.org/10.1016/j.tca.2009.06.018.
[66] G. Gbabode, P. Negrier, D. Mondieig, E. Moreno, T. Calvet, M.A. Cuevas-Diarte, Fatty acids polymorphism and solid-state miscibility. Pentadecanoic acid-hexadecanoic acid binary system, J. Alloys Compd. 469 (2009) 539–551, http://dx.doi.org/10.1016/j.jallcom.2008.02.047.
[67] F.G. Gandolfo, A. Bot, E. Flöter, Phase diagram of mixtures of stearic acid and stearyl alcohol, Thermochim. Acta 404 (2003) 9–17, http://dx.doi.org/10.1016/S0040-6031(03)00086-8.
[68] F.O. Cedeño, M.M. Prieto, A. Espina, J.R. García, Measurements of temperature and melting heat of some pure fatty acids and their binary and ternary mixtures by differential scanning calorimetry, Thermochim. Acta 369 (2001) 39–50, http://dx.doi.org/10.1016/S0040-6031(00)00752-8.
[69] K. Sato, N. Yoshimoto, M. Suzuki, M. Kobayashi, F. Kaneko, Structure and transformation in polymorphism of petroselinic acid, J. Phys. Chem. 94 (1990) 3180–3185, http://dx.doi.org/10.1021/j100370a078.
[70] K.A. Kurnia, S.P. Pinho, J.A.P. Coutinho, Designing ionic liquids for absorptive cooling, Green Chem. 16 (2014) 3741–3745, http://dx.doi.org/10.1039/C4GC00954A.
[71] G.J. Maximo, R.J.B.N. Santos, P. Brandao, J.M.S.S. Esperanca, M.C. Costa, A.J.A. Meirelles, M.G. Freire, J.A.P. Coutinho, Generating ionic liquids from ionic solids: an investigation of the melting behavior of binary mixtures of ionic liquids, Cryst. Growth Des. 14 (2014) 4270–4277, http://dx.doi.org/10.1021/cg500655s.
[72] D. Fuchs, J. Fischer, F. Tumakaka, G. Sadowski, Solubility of amino acids: influence of the pH value and the addition of alcoholic cosolvents on aqueous solubility, Ind. Eng. Chem. Res. 45 (2006) 6578–6584.